

## 0.6–3.0 wt% of Vanadium on/in Titania Monitored by X-ray Absorption Fine Structure Combined with Fluorescence Spectrometry

Yasuo Izumi,\* Fumitaka Kiyotaki, Hideaki Yoshitake,<sup>†\*</sup> Ken-ichi Aika, Tae Sugihara,<sup>††</sup> Takashi Tatsumi,<sup>††</sup>  
Yasuhiro Tanizawa,<sup>†††</sup> Takafumi Shido,<sup>†††</sup> and Yasuhiro Iwasawa<sup>†††</sup>

Interdisciplinary Graduate School of Science and Engineering, Tokyo Institute of Technology,  
4259 Nagatsuta, Midori-ku, Yokohama 226-8502

<sup>†</sup>Graduate School of Environment and Information Sciences,

Yokohama National University, Tokiwadai, Hodogaya, Yokohama 240-8501

<sup>††</sup>Graduate School of Engineering, Yokohama National University, Tokiwadai, Hodogaya, Yokohama 240-8501

<sup>†††</sup>Graduate School of Science, The University of Tokyo, Bunkyo-ku, Hongo 113-0033

(Received August 26, 2002; CL-020724)

Selective XAFS measurements of 0.6–3.0 wt% V sites on/in TiO<sub>2</sub> were enabled utilizing a fluorescence spectrometer. The V sites were V<sup>IV</sup> species in the case of high-surface-area V-TiO<sub>2</sub> in contrast to V<sup>V</sup> species in the case of conventional V/TiO<sub>2</sub> catalysts, V supported on HSA-TiO<sub>2</sub>, and V-TiO<sub>2</sub> prepared in the absence of dodecylamine (general sol-gel method).

Vanadium catalysts are used for the reduction of nitric oxide with ammonia,<sup>1</sup> the oxidation of naphthalene/*o*-xylene to phthalic anhydride, and the oxidation of butane to maleic anhydride.<sup>2</sup> The optimal catalytic performance in these applications has been reported to correspond to concentrations of V of less than a monolayer, dispersed on TiO<sub>2</sub>. When the concentration of V corresponds to monolayer levels, major V species has been proposed to be a monomeric monooxo<sup>3</sup> or dioxo vanadate,<sup>4</sup> polyvanadates<sup>3</sup> such as decavanadate ([V<sub>10</sub>O<sub>28</sub>]<sup>6-</sup>),<sup>5</sup> or to an epitaxial V<sub>2</sub>O<sub>5</sub>(010) layer over TiO<sub>2</sub><sup>6</sup> by Raman,<sup>51</sup> V NMR, UV-visible, etc.

XAFS directly determines the local structure of non-crystalline materials. However, exceptionally it is very difficult to measure XAFS data for low concentrations of V in the TiO<sub>2</sub> matrix. When 0.6 wt% of V (1.1 wt% V<sub>2</sub>O<sub>5</sub>) is mixed with TiO<sub>2</sub>, the V K-edge jump is only 0.037 compared to a total absorption of 4 in transmission mode. The photon number ratio of V Kα<sub>1</sub>/Ti Kα<sub>1</sub> is only 0.012 in fluorescence mode. When a solid-state detector (SSD; ΔE ≈ 100 eV) is used, the V Kα<sub>1</sub> (4952.2 eV) peak can be separated from the Ti Kα<sub>1</sub> (4510.8 eV) peak. However, the Ti Kβ<sub>1,3</sub> (4931.8 eV) still overlaps the V Kα<sub>1</sub>. The ratio of V Kα<sub>1</sub>/Ti Kβ<sub>1,3</sub> is 0.058. The selective detection of V Kβ<sub>1,3</sub> (5427.3 eV) is difficult using the SSD because scattered X-rays overlap. Auger or secondary photoelectrons derived from V are selectively monitored using an electron energy analyzer. However, these experiments need ultra-high vacuum, and in-situ measurements are impossible. In this Letter, XAFS combined with fluorescence spectrometry<sup>7,8</sup> was applied to selectively monitor low concentrations of V on/in TiO<sub>2</sub>.

TiO<sub>2</sub> (P25, 60 m<sup>2</sup>g<sup>-1</sup>) was impregnated with V triisopropoxide oxide (1) in isopropanol solution (V/TiO<sub>2</sub>). A high surface area (HSA; 1200 m<sup>2</sup>g<sup>-1</sup>) V-TiO<sub>2</sub> was prepared from compound 1, Ti tetraisopropoxide (2), and dodecylamine.<sup>9</sup> An aqueous solution was kept at 333 K for six days, and filtered. The obtained powder was heated at 453 K for ten days, and then washed by *p*-toluenesulfonic acid/ethanol. HSA-TiO<sub>2</sub> prepared in a similar procedure was

impregnated with compound 1 (V/HSA-TiO<sub>2</sub>). V-TiO<sub>2</sub> was prepared from compounds 1 and 2 in the absence of dodecylamine in a similar manner to the case of HSA V-TiO<sub>2</sub>. In all cases, the dried powder was heated in air at 473 K and pressed into a disk in ambient air.

The XAFS spectra were measured at KEK-PF 7C. The storage ring energy was 2.5 GeV, and the current was 390–270 mA. A Si(111) double crystal monochromator was used. The beam was focused and fully tuned. The X-ray fluorescence from the sample was analyzed using a Rowland-type spectrometer (*R* = 180 mm) equipped with a Johansson-type Ge(331) crystal and scintillation counter.<sup>7</sup> The entire beam path was in helium, except for the I<sub>0</sub> ion chamber (N<sub>2</sub> : He = 3 : 7).

The V Kα<sub>1</sub> emission spectrum was measured with the excitation energy set at 5484.1 eV. Next, the V K-edge XANES was measured. The fluorescence spectrometer was tuned to the emission peak energy (≤1000 cps). The Ge(331) crystal received a solid angle of 0.007 sr for the X-ray fluorescence from the sample. The step scan was ≈0.25 eV. The dwell time of each data point was 60–200 s. The energy position was reproduced within ±0.1 eV. The V Kα<sub>1</sub> and V K rising edge energy of the V metal were calibrated to 4952.2 and 5463.9 eV, respectively.

The V Kα<sub>1</sub> emission spectra for the V/TiO<sub>2</sub> catalysts appeared at 4951.5–4952.0 eV (Figure 1). The chemical shifts with respect to V metal were reported to –0.1, –0.3–0.4, and –0.5–0.6 eV for V<sup>III</sup>, V<sup>IV</sup>, and V<sup>V</sup> compounds, respectively.<sup>10</sup> Hence, the V sites in the catalysts are in the oxidation state of IV/V. The FWHM

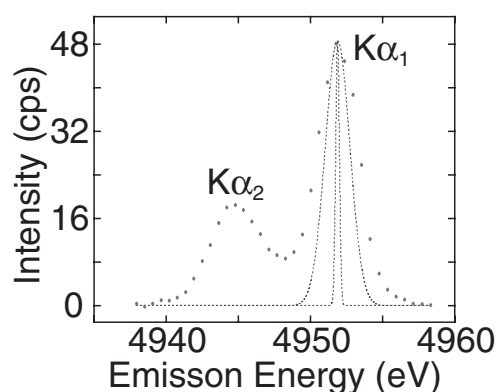


**Figure 1.** V Kα<sub>1</sub> and α<sub>2</sub> emission spectrum for V/TiO<sub>2</sub> of 3.0 wt%-V. Best energy resolution of the fluorescence spectrometer (narrower peak of dotted line) and of beamline (wider peak of dotted line) is also drawn.

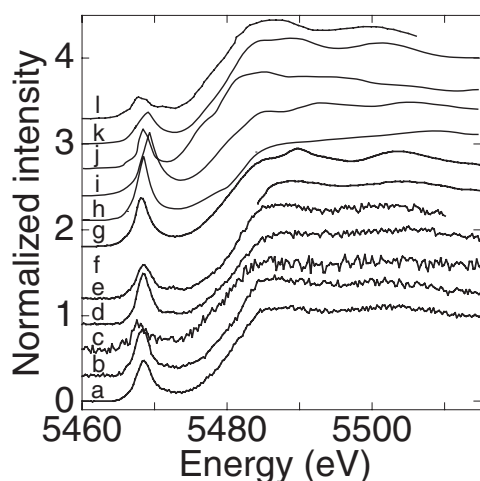


**Figure 2.** V K-edge XANES spectra for V+TiO<sub>2</sub> catalysts measured using a fluorescence spectrometer (a–c). V/TiO<sub>2</sub> of 3.0 (a) and 1.0 wt%-V (b). HSA V-TiO<sub>2</sub> (0.6 wt%-V, c). V/HSA-TiO<sub>2</sub> (1.0 wt%, d). V-TiO<sub>2</sub> (2.0 wt%, e). Reference V (f–k) and Ti K-edge (l) XANES measured in transmission mode for V/TiO<sub>2</sub> (3.9 wt%-V, f, above 5484 eV),<sup>11</sup> Mn<sub>0.90</sub>V<sub>1.80</sub>Mo<sub>0.20</sub>O<sub>6</sub> (g), CrV<sup>V</sup>O<sub>4</sub> (h),<sup>12</sup> V<sub>2</sub>O<sub>5</sub> (i),<sup>12</sup> V<sup>IV</sup>OSO<sub>4</sub>·3H<sub>2</sub>O (j),<sup>12</sup> V<sup>IV</sup><sub>2</sub>O<sub>4</sub> (k),<sup>12</sup> and HSA-TiO<sub>2</sub> (l).<sup>9</sup>

progressively decreased (3.7–2.4 eV) as the length of two slits in the Rowland circle changed from 8.0 to 2.0 mm.<sup>7</sup>

Figure 2 shows the normalized V K-edge XANES spectra. In the case of V/TiO<sub>2</sub> (a and b), the rising edge appeared at 5480.8–5481.1 eV. Two broad post-edge peak features were observed at 5489 and 5502 eV at nearly equivalent intensity. The two peak positions were similar to the cases of V/TiO<sub>2</sub> (3.9 wt%-V, f; 5489 and 5503 eV)<sup>11</sup> and Mn<sub>0.90</sub>V<sub>1.80</sub>Mo<sub>0.20</sub>O<sub>6</sub> (3) (g; 5490 and 5504 eV). The V site in compound 3 is coordinated by two nearer O atoms (1.661–1.693 Å) and three farther O atoms (1.913–2.151 Å).<sup>13</sup> A weaker shoulder at 5486 eV appeared in (b) and (g). The post-edge pattern for CrV<sup>V</sup>O<sub>4</sub> (h) and V<sup>V</sup><sub>2</sub>O<sub>5</sub> (i) was entirely different from that of (a) and (b).

A 1s–3d pre-edge peak appeared at 5468.3–5468.6 eV for V/TiO<sub>2</sub> (a and b, Table 1). The FWHM values of the pre-edge peaks were 2.5 eV, independent of the V loadings (3–1 wt%) and of the  $\Delta E$  of the fluorescence spectrometer. The pre-edge peak width is related to the core-hole lifetime width of K+M ( $\approx 1.01$  eV) and the  $\Delta E$  of the beamline, whereas the emission peak width is related to the width of K+L<sub>3</sub> (1.26 eV) and the  $\Delta E$  of the beamline+the fluorescence spectrometer. Therefore, the  $\Delta E$  of the beamline was estimated to be 2.0 eV (Figure 1) and the  $\Delta E$  of the fluorescence

**Table 1.** The Intensity and Energy Position of Pre-edge Peaks

Entry	Sample	Intensity	Energy Position (eV)
a	V/TiO <sub>2</sub> (3.0 wt%)	0.47	5468.6
b	V/TiO <sub>2</sub> (1.0 wt%)	0.53	5468.3
c	HSA V-TiO <sub>2</sub>	0.32	5467.9
d	V/HSA-TiO <sub>2</sub>	0.59	5468.5
e	V-TiO <sub>2</sub>	0.39	5468.5
g	Mn <sub>0.90</sub> V <sub>1.80</sub> Mo <sub>0.20</sub> O <sub>6</sub>	0.57	5468.2
h	CrVO <sub>4</sub>	0.82	5468.7
i	V <sub>2</sub> O <sub>5</sub>	0.79	5469.5
j	VOSO <sub>4</sub> ·3H <sub>2</sub> O	0.48	5468.7
k	V <sub>2</sub> O <sub>4</sub>	0.35	5469.3
l	HSA-TiO <sub>2</sub>	0.25	4967.7

Only the post-edge region was reported for Fig. 2f.<sup>11</sup>

spectrometer decreased from 2.8 to 0.3 eV (Figure 1) as the slit width was decreased from 8.0 to 2.0 mm.<sup>7</sup> No contribution of Ti K $\beta_{1,3}$  appeared with these energy resolution values, demonstrating entirely no contribution of Ti in Figure 2a–e.

The pre-edge peak in (a) and (b) appeared at a similar energy to the case of compound 3 (g) and CrVO<sub>4</sub> (h). The peak intensity for (a) and (b) was 57–65% of that for (h), suggesting that the V site symmetry of V/TiO<sub>2</sub> was higher than T<sub>d</sub>.

For HSA V-TiO<sub>2</sub>, the V K $\alpha_1$  emission peak position (4951.7 eV) corresponds to V<sup>IV</sup>/V<sup>V</sup> state. The rising edge position of the XANES (5479.8 eV, c) shifted by 1.0–1.3 eV toward lower energy compared to the case of V/TiO<sub>2</sub>. Two broad peak features were observed at 5487 and 5505 eV in the post-edge region, shifted by  $\pm 2$  eV from the case of V/TiO<sub>2</sub> (a and b). The post-edge pattern of VOSO<sub>4</sub>·3H<sub>2</sub>O (j) was entirely different from (c). The post-edge pattern of V<sub>2</sub>O<sub>4</sub> (k) was relatively similar to (c), but the pre-edge peak position was at higher energy by 1.4 eV. The Ti K-edge data for HSA-TiO<sub>2</sub> was compared to the V K-edge by shifting the energy by +499.8 eV (l), since the phase parameters are similar between Ti and V. Both the post-edge pattern and pre-edge peak were similar to the case of (c).

The FWHM value of the pre-edge peak at 5467.9 eV (Table 1) for HSA V-TiO<sub>2</sub> (c) was 2.3 eV, a value smaller than the case of V/TiO<sub>2</sub> (2.5 eV, a and b). This implies that HSA V-TiO<sub>2</sub> primarily consists of V<sup>IV</sup> sites rather than a mixture of V<sup>IV</sup> and V<sup>V</sup> sites. The V<sup>IV</sup> site of V<sub>2</sub>O<sub>4</sub> is coordinated by three nearer O atoms (1.76–1.87 Å) and three farther O atoms (2.01–2.05 Å). The pre-edge peak intensity of HSA V-TiO<sub>2</sub> was 91% for the case of V<sub>2</sub>O<sub>4</sub>, suggesting a slightly higher symmetry than for the case of V<sub>2</sub>O<sub>4</sub>. EXAFS combined with fluorescence spectrometry until the wavenumber of 11 Å<sup>-1</sup> gave an average V-O distance of 1.74 Å in the case of HSA V-TiO<sub>2</sub>.

The pre-edge, rising edge, and two post-edge peaks appeared at 5468.5, 5481.1–5481.3, 5487–5488, and 5501–5504 eV and the FWHM of pre-edge peak was 2.4–2.5 eV for V/HSA-TiO<sub>2</sub> (d) and V-TiO<sub>2</sub> (e), very similar to the case of V/TiO<sub>2</sub> (a and b).

The V<sup>IV</sup> sites may be substituted on the Ti sites only in the case of HSA V-TiO<sub>2</sub>, prepared from compounds 1 and 2 and dodecylamine. V<sup>V</sup> species were dominant for the other samples and major V site structure may be common due to the similarity of spectrum. Eight of ten V atoms of [V<sub>10</sub>O<sub>28</sub>]<sup>6-</sup> are coordinated by one nearer O atom (1.61 Å) and four farther O atoms (1.83–2.05 Å),<sup>14</sup> similar to the case of V site in V<sub>2</sub>O<sub>5</sub>. Relatively low calcination temperature (473 K) and ambient condition may be the reasons why monovanadate, decavanadate, and V<sub>2</sub>O<sub>5</sub> were not observed.<sup>3–6</sup>

#### References

- W. J. Stark, K. Wegner, S. E. Pratsinis, and A. Baiker, *J. Catal.*, **197**, 182 (2001).
- G. C. Bond and P. König, *J. Catal.*, **77**, 309 (1982).
- B. Olthof, A. Khodakov, A. T. Bell, and E. Iglesia, *J. Phys. Chem. B*, **104**, 1516 (2000).
- J. Haber, A. Kozłowska, and R. Kozłowski, *J. Catal.*, **102**, 52 (1986).
- G. Deo and I. E. Wachs, *J. Phys. Chem.*, **95**, 5889 (1991).
- A. Vejus and P. J. Courtine, *Solid State Chem.*, **23**, 93 (1978).
- Y. Izumi, H. Oyanagi, and H. Nagamori, *Bull. Chem. Soc. Jpn.*, **73**, 2017 (2000).
- Y. Izumi, F. Kiyotaki, T. Minato, and Y. Seida, *Anal. Chem.*, **74**, 3819 (2002).
- H. Yoshitake, T. Sugihara, and T. Tatsumi, *Chem. Mater.*, **14**, 1023 (2002).
- S. Yasuda and H. Kakiyama, *X-Ray Spectrom.*, **7**, 23 (1978).
- R. Kozłowski, R. F. Pettifer, and J. M. Thomas, *J. Phys. Chem.*, **87**, 5176 (1983).
- J. Wong, F. W. Lytle, R. P. Messmer, and D. H. Maylotte, *Phys. Rev. B*, **30**, 5596 (1984).
- R. Kozłowski and K. Stadnicka, *J. Solid State Chem.*, **39**, 271 (1981).
- H. T. Evans, Jr., *Inorg. Chem.*, **5**, 967 (1966).